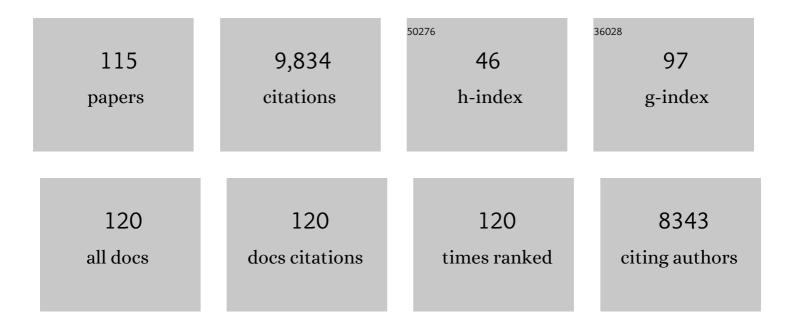
List of Publications by Year in descending order

Source: https://exaly.com/author-pdf/305746/publications.pdf Version: 2024-02-01



#	Article	IF	CITATIONS
1	Generation of intense phase-stable femtosecond hard X-ray pulse pairs. Proceedings of the National Academy of Sciences of the United States of America, 2022, 119, e2119616119.	7.1	4
2	XFEL serial crystallography reveals the room temperature structure of methyl-coenzyme M reductase. Journal of Inorganic Biochemistry, 2022, 230, 111768.	3.5	6
3	Disentangling the chemistry of Australian plant exudates from a unique historical collection. Proceedings of the National Academy of Sciences of the United States of America, 2022, 119, .	7.1	4
4	X-ray Raman Scattering: A Hard X-ray Probe of Complex Organic Systems. Chemical Reviews, 2022, 122, 12977-13005.	47.7	5
5	Carrier-specific dynamics in 2H-MoTe2 observed by femtosecond soft x-ray absorption spectroscopy using an x-ray free-electron laser. Structural Dynamics, 2021, 8, 014501.	2.3	14
6	Short-lived metal-centered excited state initiates iron-methionine photodissociation in ferrous cytochrome c. Nature Communications, 2021, 12, 1086.	12.8	17
7	Using X-ray free-electron lasers for spectroscopy of molecular catalysts and metalloenzymes. Nature Reviews Physics, 2021, 3, 264-282.	26.6	60
8	Reply to Wang et al.: Clear evidence of binding of Ox to the oxygen-evolving complex of photosystem II is best observed in the omit map. Proceedings of the National Academy of Sciences of the United States of America, 2021, 118, e2102342118.	7.1	7
9	Resonant X-ray emission spectroscopy from broadband stochastic pulses at an X-ray free electron laser. Communications Chemistry, 2021, 4, .	4.5	4
10	X-ray free-electron laser studies reveal correlated motion during isopenicillin <i>N</i> synthase catalysis. Science Advances, 2021, 7, .	10.3	23
11	Effects of x-ray free-electron laser pulse intensity on the Mn K <i>β</i> _{1,3} x-ray emission spectrum in photosystem Il—A case study for metalloprotein crystals and solutions. Structural Dynamics, 2021, 8, 064302.	2.3	10
12	Structural dynamics in the water and proton channels of photosystem II during the S2 to S3 transition. Nature Communications, 2021, 12, 6531.	12.8	73
13	Seasonal calibration of the end-cretaceous Chicxulub impact event. Scientific Reports, 2021, 11, 23704.	3.3	5
14	Near-Edge X-ray Absorption Fine Structure Spectroscopy of Heteroatomic Core-Hole States as a Probe for Nearly Indistinguishable Chemical Environments. Journal of Physical Chemistry Letters, 2020, 11, 556-561.	4.6	11
15	A new Devonian euthycarcinoid reveals the use of different respiratory strategies during the marine-to-terrestrial transition in the myriapod lineage. Royal Society Open Science, 2020, 7, 201037.	2.4	5
16	Probing a Silent Metal: A Combined X-ray Absorption and Emission Spectroscopic Study of Biologically Relevant Zinc Complexes. Inorganic Chemistry, 2020, 59, 13551-13560.	4.0	16
17	High-Resolution XFEL Structure of the Soluble Methane Monooxygenase Hydroxylase Complex with its Regulatory Component at Ambient Temperature in Two Oxidation States. Journal of the American Chemical Society, 2020, 142, 14249-14266.	13.7	41
18	Observation of Seeded Mn Kβ Stimulated X-Ray Emission Using Two-Color X-Ray Free-Electron Laser Pulses. Physical Review Letters, 2020, 125, 037404.	7.8	20

#	Article	IF	CITATIONS
19	Simultaneous Observation of Carrier-Specific Redistribution and Coherent Lattice Dynamics in 2H-MoTe ₂ with Femtosecond Core-Level Spectroscopy. ACS Nano, 2020, 14, 15829-15840.	14.6	38
20	Femtosecond electronic structure response to high intensity XFEL pulses probed by iron X-ray emission spectroscopy. Scientific Reports, 2020, 10, 16837.	3.3	13
21	Population inversion X-ray laser oscillator. Proceedings of the National Academy of Sciences of the United States of America, 2020, 117, 15511-15516.	7.1	27
22	Untangling the sequence of events during the S ₂ → S ₃ transition in photosystem II and implications for the water oxidation mechanism. Proceedings of the National Academy of Sciences of the United States of America, 2020, 117, 12624-12635.	7.1	149
23	Chemical Mapping of Ancient Artifacts and Fossils with X-Ray Spectroscopy. , 2020, , 2393-2455.		0
24	XANES and EXAFS of dilute solutions of transition metals at XFELs. Journal of Synchrotron Radiation, 2019, 26, 1716-1724.	2.4	16
25	Phonon-Suppressed Auger Scattering of Charge Carriers in Defective Two-Dimensional Transition Metal Dichalcogenides. Nano Letters, 2019, 19, 6078-6086.	9.1	43
26	Decimeter-scale mapping of carbonate-controlled trace element distribution in Neoarchean cuspate stromatolites. Geochimica Et Cosmochimica Acta, 2019, 261, 56-75.	3.9	5
27	Localized Electronic Structure of Nitrogenase FeMoco Revealed by Selenium K-Edge High Resolution X-ray Absorption Spectroscopy. Journal of the American Chemical Society, 2019, 141, 13676-13688.	13.7	47
28	Optical Control of Non-Equilibrium Phonon Dynamics. Nano Letters, 2019, 19, 4981-4989.	9.1	27
29	Double core hole valence-to-core x-ray emission spectroscopy: A theoretical exploration using time-dependent density functional theory. Journal of Chemical Physics, 2019, 151, 144114.	3.0	11
30	Carbon speciation in organic fossils using 2D to 3D x-ray Raman multispectral imaging. Science Advances, 2019, 5, eaaw5019.	10.3	35
31	Hagfish from the Cretaceous Tethys Sea and a reconciliation of the morphological–molecular conflict in early vertebrate phylogeny. Proceedings of the National Academy of Sciences of the United States of America, 2019, 116, 2146-2151.	7.1	97
32	Pheomelanin pigment remnants mapped in fossils of an extinct mammal. Nature Communications, 2019, 10, 2250.	12.8	30
33	Photons, Folios, and Fossils: The X-ray Imaging and Spectroscopy Program of Ancient Materials at SSRL. Synchrotron Radiation News, 2019, 32, 22-28.	0.8	4
34	Nouvelles spectroscopies Raman X du carbone pour les matériaux anciens. , 2019, , 22-25.	0.1	1
35	Generation of High-Power High-Intensity Short X-Ray Free-Electron-Laser Pulses. Physical Review Letters, 2018, 120, 014801.	7.8	31
36	An assessment of multimodal imaging of subsurface text in mummy cartonnage using surrogate papyrus phantoms. Heritage Science, 2018, 6, .	2.3	22

#	Article	IF	CITATIONS
37	Stimulated X-Ray Emission Spectroscopy in Transition Metal Complexes. Physical Review Letters, 2018, 120, 133203.	7.8	48
38	Structures of the intermediates of Kok's photosynthetic water oxidation clock. Nature, 2018, 563, 421-425.	27.8	386
39	A new synchrotron rapid-scanning X-ray fluorescence (SRS-XRF) imaging station at SSRL beamline 6-2. Journal of Synchrotron Radiation, 2018, 25, 1565-1573.	2.4	19
40	Probing the oxidation state of transition metal complexes: a case study on how charge and spin densities determine Mn L-edge X-ray absorption energies. Chemical Science, 2018, 9, 6813-6829.	7.4	60
41	X-ray Emission Spectroscopy as an <i>in Situ</i> Diagnostic Tool for X-ray Crystallography of Metalloproteins Using an X-ray Free-Electron Laser. Biochemistry, 2018, 57, 4629-4637.	2.5	39
42	Drop-on-demand sample delivery for studying biocatalysts in action at X-ray free-electron lasers. Nature Methods, 2017, 14, 443-449.	19.0	150
43	Metalloprotein entatic control of ligand-metal bonds quantified by ultrafast x-ray spectroscopy. Science, 2017, 356, 1276-1280.	12.6	109
44	Ligand manipulation of charge transfer excited state relaxation and spin crossover in [Fe(2,2′-bipyridine)2(CN)2]. Structural Dynamics, 2017, 4, 044030.	2.3	41
45	Soft x-ray absorption spectroscopy of metalloproteins and high-valent metal-complexes at room temperature using free-electron lasers. Structural Dynamics, 2017, 4, 054307.	2.3	34
46	Noninvasive Synchrotron-Based X-ray Raman Scattering Discriminates Carbonaceous Compounds in Ancient and Historical Materials. Analytical Chemistry, 2017, 89, 10819-10826.	6.5	27
47	Carrier-Specific Femtosecond XUV Transient Absorption of Pbl ₂ Reveals Ultrafast Nonradiative Recombination. Journal of Physical Chemistry C, 2017, 121, 27886-27893.	3.1	30
48	Ultrafast non-radiative dynamics of atomically thin MoSe2. Nature Communications, 2017, 8, 1745.	12.8	52
49	Manipulating charge transfer excited state relaxation and spin crossover in iron coordination complexes with ligand substitution. Chemical Science, 2017, 8, 515-523.	7.4	102
50	X-ray absorption spectroscopy using a self-seeded soft X-ray free-electron laser. Optics Express, 2016, 24, 22469.	3.4	19
51	Structural changes correlated with magnetic spin state isomorphism in the S ₂ state of the Mn ₄ CaO ₅ cluster in the oxygen-evolving complex of photosystem II. Chemical Science, 2016, 7, 5236-5248.	7.4	39
52	Structure of photosystem II and substrate binding at room temperature. Nature, 2016, 540, 453-457.	27.8	323
53	Elemental characterisation of melanin in feathers via synchrotron X-ray imaging and absorption spectroscopy. Scientific Reports, 2016, 6, 34002.	3.3	44
54	Observing Solvation Dynamics with Simultaneous Femtosecond X-ray Emission Spectroscopy and X-ray Scattering. Journal of Physical Chemistry B, 2016, 120, 1158-1168.	2.6	85

#	Article	IF	CITATIONS
55	Emerging Approaches in Synchrotron Studies of Materials from Cultural and Natural History Collections. Topics in Current Chemistry, 2016, 374, 7.	5.8	17
56	Geochemical Evidence of the Seasonality, Affinity and Pigmenation of Solenopora jurassica. PLoS ONE, 2015, 10, e0138305.	2.5	5
57	Bacteria or melanosomes? A geochemical analysis of micro-bodies on a tadpole from the Oligocene Enspel Formation of Germany. Palaeobiodiversity and Palaeoenvironments, 2015, 95, 33-45.	1.5	23
58	Photon-in photon-out hard X-ray spectroscopy at the Linac Coherent Light Source. Journal of Synchrotron Radiation, 2015, 22, 612-620.	2.4	35
59	The mapping and differentiation of biological and environmental elemental signatures in the fossil remains of a 50 million year old bird. Journal of Analytical Atomic Spectrometry, 2015, 30, 627-634.	3.0	28
60	Simultaneous detection of electronic structure changes from two elements of a bifunctional catalyst using wavelength-dispersive X-ray emission spectroscopy and in situ electrochemistry. Physical Chemistry Chemical Physics, 2015, 17, 8901-8912.	2.8	45
61	Bioturbating animals control the mobility of redox-sensitive trace elements in organic-rich mudstone. Geology, 2015, 43, 1007-1010.	4.4	14
62	Methods development for diffraction and spectroscopy studies of metalloenzymes at X-ray free-electron lasers. Philosophical Transactions of the Royal Society B: Biological Sciences, 2014, 369, 20130590.	4.0	23
63	Reabsorption of Soft X-Ray Emission at High X-Ray Free-Electron Laser Fluences. Physical Review Letters, 2014, 113, 153002.	7.8	33
64	Accurate macromolecular structures using minimal measurements from X-ray free-electron lasers. Nature Methods, 2014, 11, 545-548.	19.0	140
65	Tracking excited-state charge and spin dynamics in iron coordination complexes. Nature, 2014, 509, 345-348.	27.8	382
66	Synchrotron imaging reveals bone healing and remodelling strategies in extinct and extant vertebrates. Journal of the Royal Society Interface, 2014, 11, 20140277.	3.4	47
67	Taking snapshots of photosynthetic water oxidation using femtosecond X-ray diffraction and spectroscopy. Nature Communications, 2014, 5, 4371.	12.8	206
68	The Mn ₄ Ca photosynthetic water-oxidation catalyst studied by simultaneous X-ray spectroscopy and crystallography using an X-ray free-electron laser. Philosophical Transactions of the Royal Society B: Biological Sciences, 2014, 369, 20130324.	4.0	17
69	X-ray Spectroscopic Observation of an Interstitial Carbide in NifEN-Bound FeMoco Precursor. Journal of the American Chemical Society, 2013, 135, 610-612.	13.7	98
70	Stability of Pt-Modified Cu(111) in the Presence of Oxygen and Its Implication on the Overall Electronic Structure. Journal of Physical Chemistry C, 2013, 117, 16371-16380.	3.1	5
71	Experimental and Computational X-ray Emission Spectroscopy as a Direct Probe of Protonation States in Oxo-Bridged Mn ^{IV} Dimers Relevant to Redox-Active Metalloproteins. Inorganic Chemistry, 2013, 52, 12915-12922.	4.0	62
72	Metal–Ligand Covalency of Iron Complexes from High-Resolution Resonant Inelastic X-ray Scattering. Journal of the American Chemical Society, 2013, 135, 17121-17134.	13.7	75

#	Article	IF	CITATIONS
73	L-Edge X-ray Absorption Spectroscopy of Dilute Systems Relevant to Metalloproteins Using an X-ray Free-Electron Laser. Journal of Physical Chemistry Letters, 2013, 4, 3641-3647.	4.6	64
74	Simultaneous Femtosecond X-ray Spectroscopy and Diffraction of Photosystem II at Room Temperature. Science, 2013, 340, 491-495.	12.6	378
75	Synchrotron-based chemical imaging reveals plumage patterns in a 150 million year old early bird. Journal of Analytical Atomic Spectrometry, 2013, 28, 1024.	3.0	55
76	Sensitivity of X-ray Core Spectroscopy to Changes in Metal Ligation: A Systematic Study of Low-Coordinate, High-Spin Ferrous Complexes. Inorganic Chemistry, 2013, 52, 6286-6298.	4.0	35
77	Electronic Structural Changes of Mn in the Oxygen-Evolving Complex of Photosystem II during the Catalytic Cycle. Inorganic Chemistry, 2013, 52, 5642-5644.	4.0	57
78	Energy-dispersive X-ray emission spectroscopy using an X-ray free-electron laser in a shot-by-shot mode. Proceedings of the National Academy of Sciences of the United States of America, 2012, 109, 19103-19107.	7.1	113
79	Nanoflow electrospinning serial femtosecond crystallography. Acta Crystallographica Section D: Biological Crystallography, 2012, 68, 1584-1587.	2.5	167
80	Chemical Mapping of Paleontological and Archeological Artifacts with Synchrotron X-Rays. Annual Review of Analytical Chemistry, 2012, 5, 361-389.	5.4	64
81	Room temperature femtosecond X-ray diffraction of photosystem II microcrystals. Proceedings of the National Academy of Sciences of the United States of America, 2012, 109, 9721-9726.	7.1	144
82	A multi-crystal wavelength dispersive x-ray spectrometer. Review of Scientific Instruments, 2012, 83, 073114.	1.3	130
83	In situ X-ray probing reveals fingerprints of surface platinum oxide. Physical Chemistry Chemical Physics, 2011, 13, 262-266.	2.8	110
84	Manganese Kβ X-ray Emission Spectroscopy As a Probe of Metal–Ligand Interactions. Inorganic Chemistry, 2011, 50, 8397-8409.	4.0	118
85	Identification of a Single Light Atom within a Multinuclear Metal Cluster Using Valence-to-Core X-ray Emission Spectroscopy. Inorganic Chemistry, 2011, 50, 10709-10717.	4.0	68
86	X-ray Emission Spectroscopy Evidences a Central Carbon in the Nitrogenase Iron-Molybdenum Cofactor. Science, 2011, 334, 974-977.	12.6	774
87	Direct Detection of Oxygen Ligation to the Mn ₄ Ca Cluster of Photosystem II by Xâ€ray Emission Spectroscopy. Angewandte Chemie - International Edition, 2010, 49, 800-803.	13.8	78
88	The Codex of a Companion of the Prophet and the QurÄn of the Prophet. Arabica, 2010, 57, 343-436.	0.1	57
89	Probing Valence Orbital Composition with Iron KÎ ² X-ray Emission Spectroscopy. Journal of the American Chemical Society, 2010, 132, 9715-9727.	13.7	244
90	Characterization of charge transfer excitations in hexacyanomanganate(III) with Mn K-edge resonant inelastic x-ray scattering. Journal of Chemical Physics, 2010, 132, 134502.	3.0	18

UWE BERGMANN

#	Article	IF	CITATIONS
91	Complementarity between high-energy photoelectron and L-edge spectroscopy for probing the electronic structure of 5d transition metal catalysts. Physical Chemistry Chemical Physics, 2010, 12, 5694.	2.8	23
92	Mapping metals in Parkinson's and normal brain using rapid-scanning x-ray fluorescence. Physics in Medicine and Biology, 2009, 54, 651-663.	3.0	112
93	Hard X-ray Photon-In Photon-Out Spectroscopy. Synchrotron Radiation News, 2009, 22, 12-16.	0.8	29
94	Pseudo-color enhanced x-ray fluorescence imaging of the Archimedes Palimpsest. Proceedings of SPIE, 2009, , .	0.8	10
95	X-ray emission spectroscopy. Photosynthesis Research, 2009, 102, 255-266.	2.9	197
96	X-ray Emission Spectroscopy To Study Ligand Valence Orbitals in Mn Coordination Complexes. Journal of the American Chemical Society, 2009, 131, 13161-13167.	13.7	135
97	High-resolution structure of the photosynthetic Mn ₄ Ca catalyst from X-ray spectroscopy. Philosophical Transactions of the Royal Society B: Biological Sciences, 2008, 363, 1139-1147.	4.0	42
98	Nearest-neighbor oxygen distances in liquid water and ice observed by x-ray Raman based extended x-ray absorption fine structure. Journal of Chemical Physics, 2007, 127, 174504.	3.0	118
99	Archimedes brought to light. Physics World, 2007, 20, 39-42.	0.0	49
100	Resonant inelastic X-ray scattering (RIXS) spectroscopy at the Mn K absorption pre-edge—a direct probe of the 3d orbitals. Journal of Physics and Chemistry of Solids, 2005, 66, 2163-2167.	4.0	31
101	High resolution 1s core hole X-ray spectroscopy in 3d transition metal complexes—electronic and structural information. Coordination Chemistry Reviews, 2005, 249, 65-95.	18.8	830
102	X-ray damage to the Mn4Ca complex in single crystals of photosystem II: A case study for metalloprotein crystallography. Proceedings of the National Academy of Sciences of the United States of America, 2005, 102, 12047-12052.	7.1	585
103	1s2p Resonant Inelastic X-ray Scattering of Iron Oxides. Journal of Physical Chemistry B, 2005, 109, 20751-20762.	2.6	108
104	High-Resolution X-ray Emission Spectroscopy of Molybdenum Compounds. Inorganic Chemistry, 2005, 44, 2579-2581.	4.0	22
105	X-ray Absorption Spectroscopy Study of the Hydrogen Bond Network in the Bulk Water of Aqueous Solutions. Journal of Physical Chemistry A, 2005, 109, 5995-6002.	2.5	156
106	Mn oxidation states in tri- and tetra-nuclear Mn compounds structurally relevant to photosystem II: Mn K-edge X-ray absorption and K? X-ray emission spectroscopy studies. Physical Chemistry Chemical Physics, 2004, 6, 4864.	2.8	35
107	The Electronic Structure of Mn in Oxides, Coordination Complexes, and the Oxygen-Evolving Complex of Photosystem II Studied by Resonant Inelastic X-ray Scattering. Journal of the American Chemical Society, 2004, 126, 9946-9959.	13.7	177

108 Electronic Structure of Ni Complexes by X-ray Resonance Raman Spectroscopy (Resonant Inelastic) Tj ETQq0 0 0 rgBT_/Overlogt 10 Tf 50

#	Article	IF	CITATIONS
109	Site-Selective EXAFS in Mixed-Valence Compounds Using High-Resolution Fluorescence Detection:  A Study of Iron in Prussian Blue. Inorganic Chemistry, 2002, 41, 3121-3127.	4.0	95
110	Absence of Mn-Centered Oxidation in the S2→ S3Transition: Implications for the Mechanism of Photosynthetic Water Oxidation. Journal of the American Chemical Society, 2001, 123, 7804-7820.	13.7	295
111	Mn K-Edge XANES and Kl² XES Studies of Two Mnâ^'Oxo Binuclear Complexes:Â Investigation of Three Different Oxidation States Relevant to the Oxygen-Evolving Complex of Photosystem II. Journal of the American Chemical Society, 2001, 123, 7031-7039.	13.7	94
112	High-resolution X-ray spectroscopy of rare events: a different look at local structure and chemistry. Journal of Synchrotron Radiation, 2001, 8, 199-203.	2.4	45
113	Structural Investigations of Li[sub 1.5+x]Na[sub 0.5]MnO[sub 2.85]I[sub 0.12] Electrodes by Mn X-Ray Absorption Near Edge Spectroscopy. Journal of the Electrochemical Society, 2000, 147, 395.	2.9	24
114	Electronic Structure of Chemically-Prepared LixMn2O4Determined by Mn X-ray Absorption and Emission Spectroscopies. Journal of Physical Chemistry B, 2000, 104, 9587-9596.	2.6	36
115	High-resolution large-acceptance analyzer for x-ray fluorescence and Raman spectroscopy. , 1998, , .		76